Recombination profiles in poly[2-methoxy-5-(2-ethylhexyloxy)-1,4-phenylenevinylene] light-emitting electrochemical cells

J. M. Leger, S. A. Carter, and B. Ruhstaller

Citation: Journal of Applied Physics **98**, 124907 (2005); doi: 10.1063/1.2149162
View online: http://dx.doi.org/10.1063/1.2149162
View Table of Contents: http://scitation.aip.org/content/aip/journal/jap/98/12?ver=pdfcov
Published by the AIP Publishing

Recombination profiles in poly[2-methoxy-5-(2-ethylhexyloxy)-1,4-phenylenevinylene] light-emitting electrochemical cells

J. M. Leger and S. A. Carter[a)]
Department of Physics, University of California, Santa Cruz, California 95064

B. Ruhstaller
Center for Computational Physics, Zurich University of Applied Sciences, Wildbachstrasse 21, 8401 Winterthur, Switzerland

(Received 14 April 2005; accepted 11 November 2005; published online 30 December 2005)

We present a study on the optical and electronic properties of light-emitting electrochemical cells (LECs) based on poly[2-methoxy-5-(2-ethylhexyloxy)-1,4-phenylenevinylene] (MEH-PPV) with the goal of understanding emission profiles and characterizing salt and electrode dependence. Direct imaging of photoluminescence and electroluminescence profiles of planar LECs and simulations of optical interference effects were performed in order to gain insight into emission profiles in vertical structure LECs. While our results are consistent with oxidative doping, they imply a lack of reductive doping in LECs under normal operating conditions. We observe that trends in emission profiles are independent of thickness, salt, and electrode type. In addition, device current-voltage (I-V) and radiance characteristics were measured as a function of salt and electrode type. Variations in the I-V characteristics, turn-on voltage, and rectification are observed for devices with Al versus. Au contacts and for salts with varied cation type. Finally, we discuss the implications of our findings on the operating mechanism of LECs. © *2005 American Institute of Physics*.
[DOI: 10.1063/1.2149162]

INTRODUCTION

Polymer light-emitting electrochemical cells (LECs) were introduced by Pei *et al.*[1] in 1995. In a LEC, a thin film of light-emitting polymer admixed with an ionic conductor (typically polyethylene oxide, or PEO) and a salt, is sandwiched between two electrodes. According to the initial proposed operating mechanism, an applied voltage leads to electrochemical doping of the polymer, *p* type near the anode and *n* type near the cathode, leading to the *in situ* creation of a light-emitting *pn* junction.[1,2] Charge injection is then facilitated through the creation of Ohmic contacts between the electrodes and the highly conductive doped states of the polymer. The LEC was shown to operate in both forward and reverse bias, effectively independent of the electrode work function, at voltages just above the polymer band gap, consistent with the properties expected from a dynamically reversible *pn* junction.[1–5]

In 1998, deMello *et al.* proposed an alternate theory also capable of explaining these observed properties of the LEC.[6] They claimed that the accumulation of ions at the electrode–polymer interfaces introduces large electric fields that reduce the barriers to charge injection.[6,7] Thus electrochemical doping is not responsible for charge injection in the LEC. Further, they claim that any electrochemical doping present in a LEC under normal operation is unlikely.[6] Subsequent studies reporting direct photoluminescence (PL) and electroluminescence (EL) imaging in planar LEC structures, however, show a region of quenched PL that clearly indicates the presence of doped polymer.[2,8–10] These results would seem to suggest that the model presented by Pei *et al.* is the more likely picture; however, direct evidence that this model is accurate and complete is still lacking.

Recently, we have presented an in-depth study of electrochemical doping in MEH-PPV,[11] one of the most commonly used light-emitting polymers for LEC studies. We have shown that while *p* doping of this material is highly reversible, efficient, and effectively independent of anion type, *n* doping in MEH-PPV is characterized by low efficiency in most cases and inherent instability in all cases. Further, it has been shown that lithium salts are effectively incapable of *n* doping MEH-PPV using acetonitrile at room temperature,[11] an observation supported by the observation that *n* doping with alkali salts in polythiophenes and polyacetylene is not possible except when the ionic radius is increased with judicious solvent selection.[12,13] Lithium triflate is the primary salt used in studies of polymer LECs. It is thus highly doubtful that doping is strictly necessary for the operation of typical MEH-PPV LECs, such as those presented in many previous works. Indeed, convincing evidence of *n* doping in a LEC or pLEC structure at room temperature has yet to be presented. Clearly, further clarification concerning the fundamental operating mechanism is necessary for a full understanding of the polymer light-emitting electrochemical cell.

Light-emitting electrochemical cells have been systematically explored surprisingly little, considering their potential for use in air-stable displays and the controversy surrounding their operating mechanism. Experimental results have been limited primarily to a single structure (ITO/polymer:PEO:Li salt/Al). In particular, there have been limited systematic studies done on the effects of different

[a)]Author to whom correspondence should be addressed; electronic mail: sacarter@ucsc.edu

salts[14,15] and electrode materials[16] on the electrical and optical properties of the LEC. Finally, planar structures have been well studied but the results obtained for these structures have not been correlated to trends in vertical structure LECs to allow the generalization of these important results.

In this work, we built both vertical and planar geometry LECs using MEH-PPV as the emissive material. Devices were varied by salt type, salt concentration, operating voltage, and electrode type. For the planar devices, *in situ* photoluminescence and electroluminescence profiles were directly imaged using a confocal microscope and CCD camera. For the vertical geometry devices, EL spectra are measured in both forward and reverse bias, in addition to typical current-voltage and radiance-voltage characterization. We use simulations of interference effects in multilayered device structures using parameters obtained by observing emission profiles in pLECs to predict emission profiles and compare with experimental results. Finally, we discuss implications regarding the underlying operating mechanism of the LEC.

EXPERIMENT

Both planar and vertical geometry LECs were constructed using MEH-PPV provided by American Dye Source as the emissive material. All polymer solutions consisted of MEH-PPV and PEO in a 9:4 ratio, and salt in varying amounts, in chlorobenzene. Salts used include lithium trifluoromethanesulfonate (triflate), tetrabutylammonium (TBA) tetrafluoroborate (BF_4), TBA hexafluorophosphate (PF6), and TBA-triflate. Planar geometry LECs used a lower molecular weight (~100 000) PEO to minimize phase separation while the vertical geometry LECs used a higher molecular weight (~5 000 000) PEO to achieve thicker films. After spin casting, films were annealed at 80 °C for 3 min in an inert atmosphere, and placed under vacuum ($\sim 10^{-7}$ Torr) overnight. Film thicknesses were measured on a Park Scientific Autoprobe CP Atomic Force Microscope (AFM) and showed a variation of ±15 nm.

Planar geometry LECs were fabricated by evaporating gold strips onto glass substrates after prior masking with a 15 μm fine wire. Carefully removing the wire resulted in a clean gap of ~20 μm thickness, as determined by AFM. A polymer solution was then spin cast onto the substrate, annealed at 80 °C for 3 min in an inert atmosphere, and placed under vacuum ($\sim 10^{-7}$ Torr) overnight. Prior to testing, the devices were encapsulated under inert atmosphere under a glass slide using Addison Clear Wave AC A1425 UV curable epoxy and UV cured in air. Contact to the electrodes was made using copper tape with conducting adhesive. Images of PL and EL were obtained using a 40× oil immersion lens on a Technical Instruments K2 SBIO confocal microscope with a QImaging micropublisher CCD camera. The photoluminescence source was an Osram HBO-100 W/2 mercury short arc photo optic lamp with a rhodamine filter.

The vertical geometry LEC devices were prepared by spin casting the polymer solution to a thickness of ~350 nm onto prepatterned ITO glass substrates. Top electrodes were deposited by thermal evaporation. All device testing took place in a dry nitrogen glove box using a Keithley 2400 sourcemeter, a picoammeter, and a calibrated silicon photodetector. Electroluminescence spectra were also taken in an inert nitrogen atmosphere with an Ocean Optics fiber optic spectrometer.

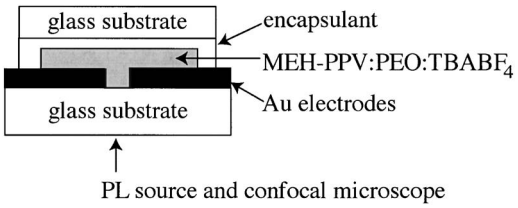

FIG. 1. Device structure of a planar geometry light-emitting electrochemical cell.

PLANAR GEOMETRY LECS

Planar geometry LECs were constructed as shown in Fig. 1 using various salt types and with an average width of ~20 μm. Images of the device photoluminescence and electroluminescence profiles were captured using a confocal microscope and CCD camera, as described above. We found that the salt type made little difference in the general results despite significant differences in the type and size of the anions ($triflate^-$ vs BF_4^-) and cations (Li^+ vs TBA^+). The 0 V photoluminescence, 3 V bias photoluminescence, and electroluminescence at 10 V of a representative device are shown in Fig. 2.

As the applied voltage is increased, PL quenching can be observed at the anode beginning as low as 1 V, indicating

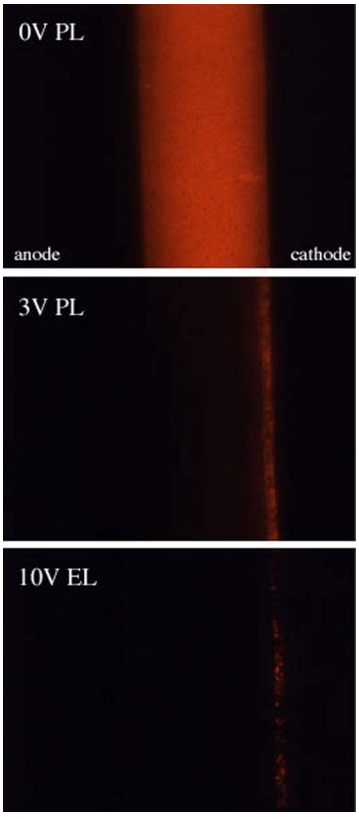

FIG. 2. (Color online) The 0 V photoluminescence, 3 V photoluminescence, and 10 V electroluminescence of a planar LEC with $TBABF_4$ salt.

oxidative doping. Edman *et al.* show that the onset of *p*-type doping at voltages well below the band gap of the material in planar LEC structures is due to the location of the gold work function relative to the HOMO/LUMO levels of the polymer.[17] Of particular interest is the observation that no evidence of PL quenching occurs at the cathode, suggesting a lack of reductive doping in the device under normal operation. Previous groups have suggested that the lack of distinct PL quenching at the cathode is due rather to low concentrations of doped material or that PL quenching may be less efficient in an *n* doped than in a *p*-doped polymer, although a clear argument is not given in either case.[2,10]

At 3 V, the PL is highly quenched to within ~10% of the polymer layer thickness from the cathode. As the bias is increased, the quenched region moves toward the cathode, as noted by other groups. The precise location of the quenched/unquenched interface varied significantly from device to device but occurred typically between 10%–40% of the device width away from the cathode. It is possible that this location is highly sensitive to variations in salt concentration. The devices with emission occurring closer to the center of the device typically were less bright and less uniform than those with emission near the cathode and thus were less well suited for imaging. The reasons for this observed trend are currently unclear. In our findings, the region of EL always occurred on the anode-side edge of the unquenched region with a characteristic width of ~1/14–1/16 of the device thickness. This could be due to the creation of a *pn* junction within the device, or could suggest that charge recombination may be limited by hole injection from the *p*-doped polymer into the undoped region.

The ability to directly image the photoluminescence and electroluminescence profiles of planar LEC structures has provided very important information that may help us to understand the operating mechanism of LECs. It is reasonable to assume that, in general, the devices in planar and vertical geometry operate under the same basic principles;[18] however, observations of planar devices are limited in several important respects. First, the planar devices necessarily are restricted to using the same material for both electrodes, disallowing the study of device operation in the presence of a built-in electric field. Second, the imaging of these devices takes place outside the inert atmosphere due to the necessity of using a microscope for fine imaging. This requires some kind of encapsulation and exposure to air, both of which may affect device operation and prevent the successful study of devices with electrodes that are oxygen sensitive, such as Al or Ag. Studies have been presented using nonencapsulated devices built and tested under inert atmosphere.[9] However, these devices were necessarily large-area (~1.5 mm) to avoid the necessity of using a microscope for imaging and therefore required extremely high operating voltages (~400 V).

Finally, the construction of devices with such drastically different geometries may result in a very different electric field profile within the device. In order to make conclusions from the observations of planar LECs we desire some evidence that the basic observed properties of the planar devices are duplicated in the vertical devices, and then extend the study to include devices with variations in thickness and electrode work functions. Unfortunately, the vertical geometry prevents the direct observation of emission and photoluminescence profiles, requiring the study of these properties via a less direct approach.

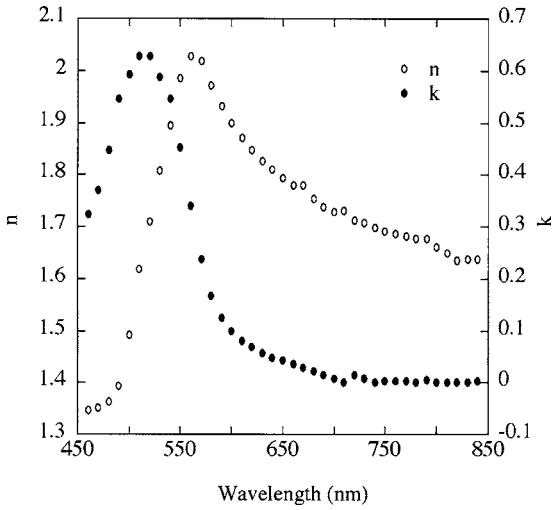

FIG. 3. Optical constants *n* and *k* of a thin film of MEH-PPV:PEO.

SIMULATING INTERFERENCE EFFECTS IN VERTICAL GEOMETRY LECS

In order to investigate emission profiles in vertical geometry LECs, we performed simulations that model interference effects in single layer polymer light-emitting device structures (ETFOS Emissive Thin Film Optics Simulator provided by Ruhstaller). Since polymer LECs consist of a multilayer thin film stack with a total thickness on the order of the emission wavelength, the emission spectra critically depend on the charge recombination profile within the polymer layer, in addition to the layer thicknesses and refractive indices of the individual layers. In previous work, we used simulations of interference effects to investigate the dependence of polymer light-emitting diodes on polymer layer thickness.[19] The simulation technique is based on a transfer matrix formalism with an oscillating point dipole source and is described in further detail there.

The simulation parameters thickness, basis spectra, refractive index, and emission profile were determined experimentally. In particular, the layer thicknesses of our experimental devices were measured with AFM and the resulting values used in simulation. We use the EL spectrum of a very thin (30 nm) MEH-PPV LED as the emission spectrum of the dipole. The spectral features of such a thin device were found to be effectively independent of interference effects, as determined via simulation, and thus suitable as a basis spectrum for this application. The refractive index dispersion curves of MEH-PPV:PEO were measured by spectroscopic ellipsometry (VASE by Woollam Inc.) and are shown in Fig. 3. The refractive index measurement was performed on films without salt in order to improve film uniformity for the measurement. The transmission and reflection characteristics of films with and without salts were compared and found to be

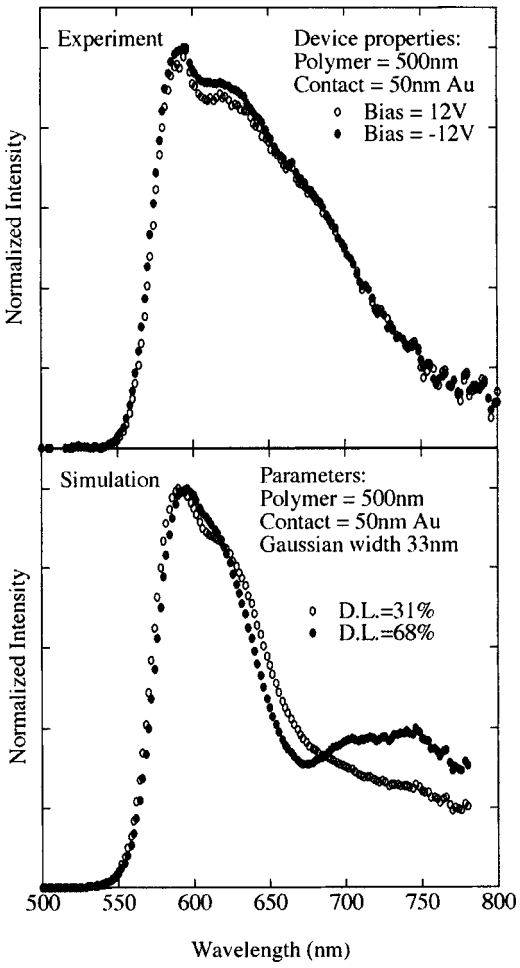

FIG. 4. Experimental and simulated EL spectra of a 500 nm device with Au top electrodes in forward and reverse bias. D.L.=Emissive dipole location as a function of layer thickness relative to the top electrode.

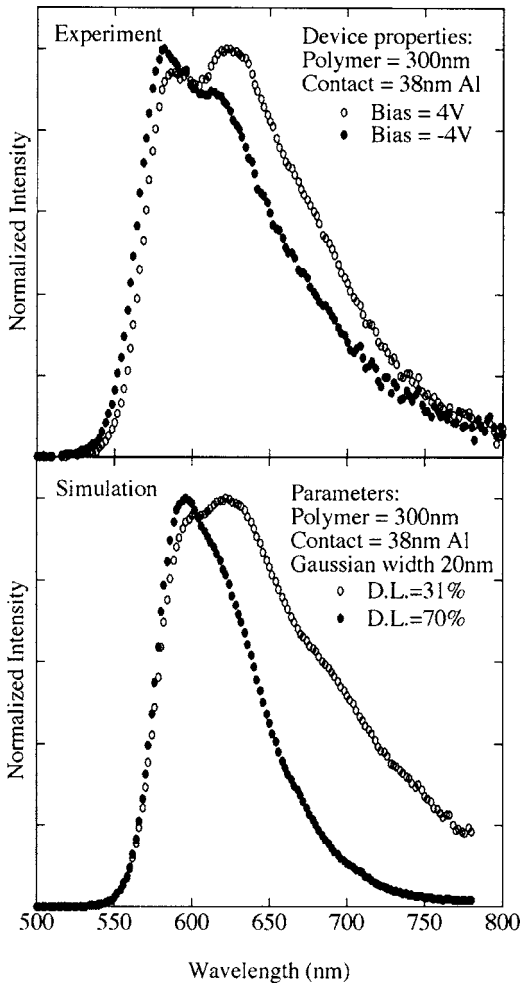

FIG. 5. Experimental and simulated EL spectra of a 300 nm device with Al top electrodes in forward and reverse bias.

identical within error, suggesting that the refractive indices determined using this method are a good approximation to those of a typical LEC film.

For the emission profile, we use a Gaussian distribution of dipole locations with a characteristic width of 1/15 of the polymer layer thickness. This value was obtained by observing the typical width of the EL emission in our planar LEC devices. We make the assumption that the width of the emission profile scales with device thickness, as observed by others.[9] After defining the parameters within the simulation software to match those measured for the experimental device, spectra were generated assuming a dipole location specified as a percentage of the polymer layer thickness relative to the interface with the evaporated top electrode.

COMPARISON OF SIMULATION AND EXPERIMENT: EL SPECTRA OF MEH-PPV LECS

The experimental and most closely matched simulated EL spectra for three different devices and various operating voltages are shown in Figs. 4–7. Figure 4 compares spectra for a 500 nm device with Au top electrodes and Fig. 5 shows similar results for a 300 nm device with Al top electrodes. In both cases, the best simulation results were obtained by assuming the location of light emission to be approximately 30% of the device thickness away from the cathode for both forward and reverse bias. It should be noted that, as with the planar LECs, no noticeable dependence of the emission profiles were observed for variations in salt type.

Figures 6 and 7 compare experimental and simulated EL spectra for a 250 nm thick device with Au top electrodes. Figure 6 shows forward and reverse bias while Fig. 7 shows spectra for high and low reverse bias voltages. For this device, emission occurs symmetrically at approximately 10% of the layer thickness away from the electrodes and shifts toward the cathode by about 4% of the polymer layer thickness upon increasing the applied voltage from −4 to −8 V.

The precise location of the symmetric light emission as a fraction of the polymer layer with respect to the electrodes varies a significant amount for each simulated device but typically fell in the range of 10% to 30%. This number clearly varied with the applied voltages at which the spectra were obtained, but also varied significantly from device to device, suggesting that the location of light emission in a given device is highly sensitive to slight changes in the device preparation. We observed no systematic thickness dependence in emission location as a percentage of layer thickness. The differences in the results of Figs. 4 and 6 represent the typical device to device variation.

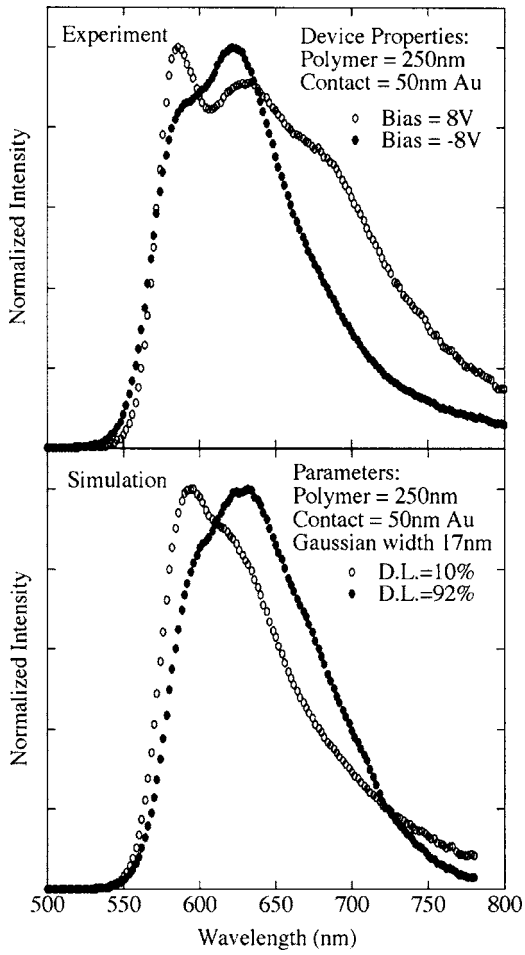

FIG. 6. Experimental and simulated EL spectra of a 250 nm device with Au top electrodes in forward and reverse bias.

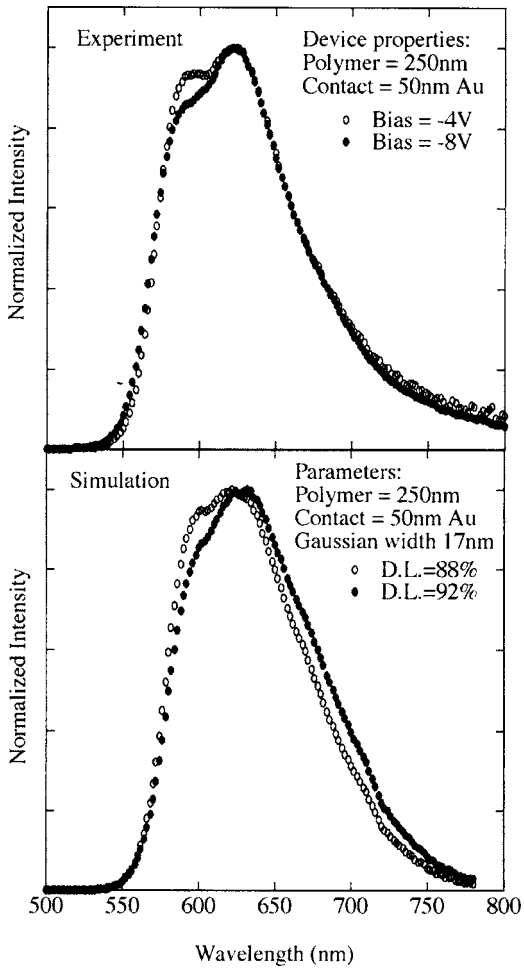

FIG. 7. Experimental and simulated EL spectra of a 250 nm device with Au top electrodes in high and low reverse bias.

It should be noted that the variation in the emission location for the vertical structure LECs as determined by simulation is of a similar range as the variation seen for the planar structures. For reference, Fig. 8 shows simulated EL spectra for a 300 nm device with an Al top electrode as a function of the dipole location within the device. The variation is quite dramatic and in nearly all cases the match to the experimental spectra for a given voltage was unique to one specific emission location. We can therefore assume that the predicted emission locations are correct.

In general, the comparison between the experimental voltage-dependent EL spectra and simulations of these spectra show excellent correlation when we assume a Gaussian dipole emission with a characteristic width of about 1/15 of the polymer layer thickness centered an approximately equal distance from the cathode and anode in forward and reverse bias, respectively. These results therefore reproduce the trends in the emission profile as determined experimentally for the planar devices for each device. Further, they indicate that the voltage-dependent trends in emission profiles are general with respect to polymer layer thickness and top electrode work function. The simulation of optical interference effects in vertical geometry polymer light-emitting electrochemical cells therefore show remarkably strong evidence that the various results demonstrated for planar structure LECs can be generalized to vertical structure devices.

ELECTRICAL AND OPTICAL CHARACTERIZATION OF VERTICAL GEOMETRY LECS

In order to further characterize our vertical geometry LECs with respect to top electrode and salt type, we took

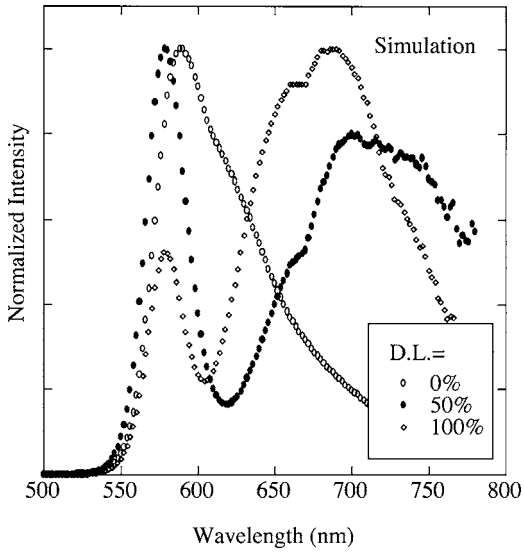

FIG. 8. Simulated EL spectra of a 300 nm device with Al top electrodes as a function of emission location throughout the polymer layer.

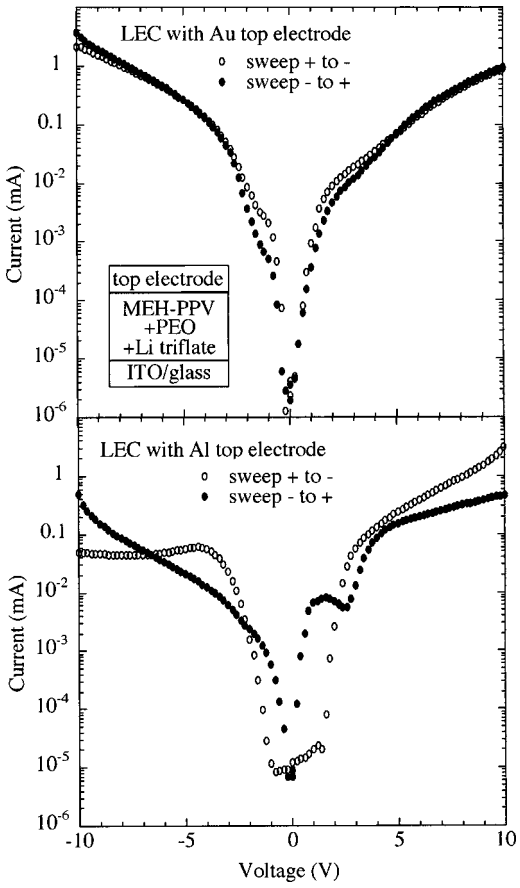

FIG. 9. Current-voltage curves for LECs using Li triflate and both Au and Al top electrodes. Devices were first charged at high positive or negative voltages prior to voltage sweep.

current-voltage and radiance curves for several device configurations. In general, the I-V characteristics of these devices were sensitive to the specific scanning procedure. Consistent results were obtained from scans performed,starting from the maximum positive or negative scan voltage and swept to the other extreme. The devices were held at the maximum range of positive or negative voltages until stable light output was achieved (several seconds to one minute) prior to scanning in order to compensate for the initial time required for the ions to move through the polymer film and establish a doping profile. It is important to note that this initial charging in no way establishes a permanent or semipermanent doping profile within the polymer layer. A 1.5 s delay between voltage step and current-radiance measurement was introduced to compensate for the slow ion mobility through the polymer film.

Typical I-V curves for a vertical structure LEC with Au and Al top electrodes are shown in Fig. 9. Using an Au top electrode, the devices display remarkably symmetric I-V characteristics that are similar in shape to a typical polymer LED in forward bias and are effectively independent of the direction of the scan. For the device with Al top electrode, however, the I-V curves show a much stronger dependence on the scan direction.

In our previous study, we showed that the reversibility of oxidation in MEH-PPV depended strongly on the tendency of the electrode on which the doping took place to oxidize.

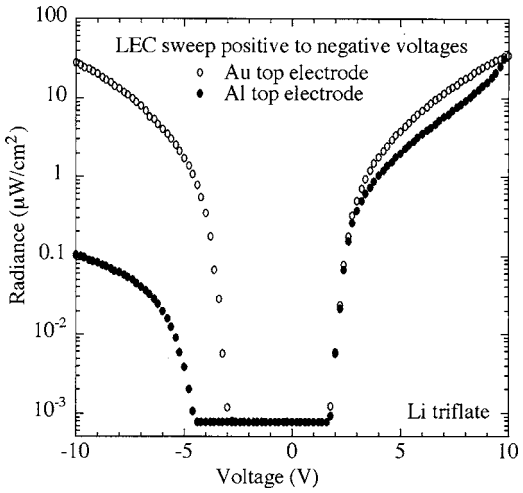

FIG. 10. Radiance-voltage curves for devices using Li triflate and Au or Al top electrodes.

Specifically, the reversibility of *p* doping in MEH-PPV films on Al substrates in an oxygen-educed, but not inert, atmosphere was very low. When charging in forward bias, the oxidation takes place at the ITO interface. As the scan reaches high negative potentials, the current decreases, possibly due to some oxidation occurring of the Al electrode. When charging at negative voltages, oxidation occurs at the Al interface. Presumably the low oxygen levels present in the inert atmosphere result in only a limited oxide layer on the Al and thus in steady-state reverse bias the device current is uncompromised. As the device is scanned to positive voltages, a feature appears in the I-V curve that may be attributed to the reversal of the oxidation in the Al electrode that results in a temporary decrease in the device current.

Figure 10 shows radiance-voltage curves for two LEC devices with Au and Al top electrodes. The device with an Au top electrode showed lower turn-on voltages in reverse bias than the device with an Al top electrode, also indicating a possible process such as oxidation of our top electrode in reverse bias, occurring for Al but not for Au. Although the devices were placed in high vacuum overnight and tested in an inert nitrogen atmosphere, evidence suggests the presence of some minor oxide formation of the Al contacts in both the I-V and radiance data. If the differences in these devices were due simply to the difference in electrode work functions, we would expect to see more straightforward differences in the I-V and radiance characterization such as similar shapes but shifted turn-on voltages in both directions. This sensitivity of the device behavior to the presence of minor amounts of oxygen has implications for the light-emitting displays constructed using top electrodes such as Al or Ag that are intended to increase the air stability of polymer devices over those that employ reactive high work function top electrodes such as Ca.

Figure 11 shows the radiance curves for LECs with various salts. The device made using Li triflate shows much lower turn-on voltages in reverse bias than those with TBA cations when scanning from positive to negative voltages. It is possible that the tendency of the TBA cation to reduce ITO

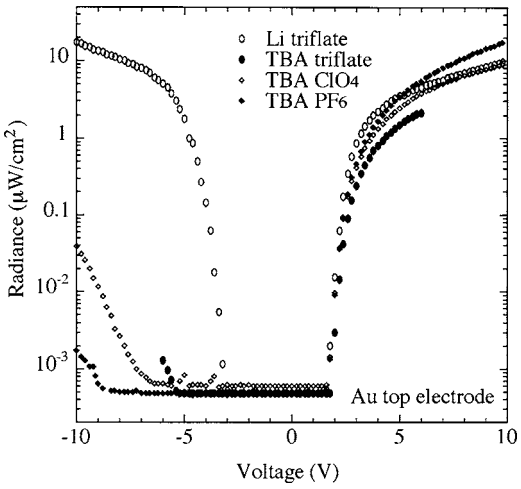

FIG. 11. Radiance-voltage curves for devices using various salts and Au top electrodes.

at voltages lower than those necessary to reduce MEH-PPV or a reduced mobility of the TBA cation could be affecting the device turn-on in reverse bias.

DISCUSSION AND CONCLUSIONS

We have reported on a study on MEH-PPV based light-emitting electrochemical cells that includes a study of the emission profiles in both planar and vertical structure LECs and systematically explores the device performance in LECs with various salt types and top electrode metals. Planar geometry LECs were constructed and their photoluminescence and electroluminescence profiles were directly imaged. Our results confirm previously reported studies that *p* doping occurs at voltages well below the polymer band gap,[11] that EL occurs with a characteristic width at the edge of the region with unquenched PL and shifts toward the cathode with increased voltages, and that no clear evidence of *n* doping is seen under normal operating conditions, even with TBA salts, which have been shown to be effective in *n*-doping MEH-PPV.

We performed simulations of optical interference effects in multilayered device structures to predict emission profiles in vertical structure LECs and found that the results correlated surprisingly well with those results presented for planar devices. We showed further that these results are general with respect to polymer layer thickness, top electrode choice, and salt type.

Finally, we characterized the optical and electronic properties of LECs and found that the I-V characteristics and light emission depend strongly on the choice of top electrode and salt cation. In particular, devices with Au top electrodes and Li salts show highly symmetric diode-like I-V curves and symmetric turn-on behavior. Devices with Al top electrodes show sensitivity to oxidation of the top contact even when tested in an inert atmosphere that affects the I-V curves and causes delayed emission in reverse bias. Devices using TBA salts also show delayed and reduced emission in reverse bias.

Recent results in the study of the electrochemical doping process in MEH-PPV have highlighted the need to revisit the issue of the operating mechanism of the LEC for which electrochemical doping is thought to be central to the operation of the device. The results of studies on planar LECs under normal operating conditions in combination with studies showing that Li triflate, a commonly used salt in LEC applications, does not *n* dope MEH-PPV in most cases, suggest that*n* doping is not strictly necessary for the operation of the LEC. The simulation results allow us to generalize these results to vertical LECs with a variety of salts and electrodes. We strongly suspect that the inclusion of dipole effects at the polymer–cathode interface are, in fact, necessary to fully explain the efficient electron injection seen in these devices and to accurately model the LEC operating mechanism.

ACKNOWLEDGMENTS

We gratefully acknowledge support from NSF ECS Grant No. 0101794. We wish to thank J.C. Scott at IBM Almaden for his assistance in the measurements of the optical constants of our polymer films.

[1]Q. Pei, G. Yu, C. Zhang, Y. Yang, and A. J. Heeger, Science **269**, 1086 (1995).
[2]Q. Pei, Y. Yang, G. Yu, C. Zhang, and A. J. Heeger, J. Am. Chem. Soc. **118**, 3922 (1996).
[3]Y. Li, Y. Cao, J. Gao, D. Wang, G. Yu, and A. J. Heeger, Synth. Met. **99**, 243 (1999).
[4]D. L. Smith, J. Appl. Phys. **81**, 2869 (1997).
[5]I. Riess and D. Cahen, J. Appl. Phys. **82**, 3147 (1997).
[6]J. C. DeMello, N. Tessler, S. C. Graham, and R. H. Friend, Phys. Rev. B **57**, 12951 (1998).
[7]J. C. DeMello, J. J. M. Halls, S. C. Graham, N. Tessler, and R. H. Friend, Phys. Rev. Lett. **85**, 421 (2000).
[8]D. J. Dick, A. J. Heeger, Y. Yang, and Q. Pei, Adv. Mater. (Weinheim, Ger.) **8**, 985 (1996).
[9]J. Gao and J. Dane, Appl. Phys. Lett. **83**, 3027 (2003).
[10]J. Gao and J. Dane, Appl. Phys. Lett. **84**, 2778 (2004).
[11]A. L. Holt, J. M. Leger, and S. A. Carter, J. Chem. Phys. **123**, 044704 (2005).
[12]M. Mastragostino and L. Soddu, Electrochim. Acta **35**, 463 (1990).
[13]G. Zotti, G. Schiavon, and S. Zecchin, Synth. Met. **72**, 275 (1995).
[14]Y. Cao, Q. B. Pei, M. R. Andersson, G. Yu, and A. J. Heeger, J. Electrochem. Soc. **144**, L317 (1997).
[15]L. Edman, D. Moses, and A. J. Heeger, Synth. Met. **138**, 441 (2003).
[16]Q. Sun, C. Yang, G. He, Y. Li, and H. Wang, Synth. Met. **138**, 561 (2003).
[17]L. Edman, M. A. Summers, S. K. Burratto, and A. J. Heeger, Phys. Rev. B **70**, 115212 (2004).
[18]F. P. Wenzl, P. Pachler, E. J. W. List, D. Somitsch, P. Knoll, S. Patil, R. Guentner, U. Scherf, and G. Leising, Physica E (Amsterdam) **13**, 1251 (2002).
[19]J. M. Leger, B. Ruhstaller, H. G. Nothofer, U. Scherf, H. Tillman, H. H. Horhold, and S. A. Carter, Phys. Rev. B **68**, 054209 (2003).